PERGAMON

Solid State Communications 118 (2001) 361–365

solid state communications

www.elsevier.com/locate/ssc

Predicted scanning tunneling microscopy images of carbon nanotubes with atomic vacancies

Arkady V. Krasheninnikov*

Moscow State Engineering Physics Institute (Technical University), Kashirskoe shosse 31, 115409 Moscow, Russia

Received 26 January 2001; accepted 16 February 2001 by J.F. Sadoc

Abstract

We calculated STM images of both metallic and semiconducting single-wall carbon nanotubes with atomic vacancies. In our simulations, we employed the tight-binding Green's function technique and the recursion method. We predict that vacancies should result in the formation of hillock-like features in STM images of metallic nanotubes, which are especially appreciable at small bias voltages (of about 0.1–0.4 V). An enhancement in the tunneling current is due to vacancy-induced states at the Fermi energy, and these states are spatially localized on the atoms surrounding the vacancies. Electronic superstructures analogous to those in graphite near point defects are observed near the vacancy. For semiconducting nanotubes, hillocks and superstructures are also visible at those bias voltages when band edges contribute to the tunneling current.

PACS: 81.07.De; 73.22.-f; 87.64.Dz

Keywords: A. Fullerenes; C. Point defects; C. Scanning tunneling microscopy; D. Electronic states (localized)

Although carbon nanotubes (NTs) have been considered as ideal defect-free objects in the vast majority of theoretical works, NTs may have various atomic-scale point defects. Examples of those are pentagon/heptagon topological defects, [1,2,3] adatoms [4] on the walls of NTs and atomic vacancies, [5,6,7] all of which can appear during NT growth or can be created by external actions, e.g., by irradiation. Studies on NTs with defects present considerable interest in themselves as well as with a view toward understanding electronic transport [5,6,7,8,9] in these quasi-one-dimensional conductors.

Recent experiments evidence that high-dose electron [10,11] and Ar ion [12] irradiation of NTs gives rise to the formation of irradiation-induced defects, surface reconstructions and drastic dimensional changes, as a corollary of which the apparent diameter of NTs substantially shrinks.

However, particular types of irradiation-induced defects have not been yet specified. It has been suggested [11] that isolated vacancies appear under irradiation, but such defects are unstable and the apparent reduction of the NT diameter is due to a mending of the vacancies through dangling bond saturation.

On the other hand, appearances of surface dangling bonds in irradiated NTs have been reported [12]. Since dangling bonds are usually associated with isolated vacancies, such vacancies, even if metastable, may be long-lived defects (and may survive for macroscopic times), especially under low-temperature, low-dose irradiation. Thus, the stability of vacancies and their influence on the electronic properties of NTs call for further studies.

Scanning-tunneling microscopy (STM) is a perfect tool to study atom-scale defects in NTs since this technique enables one to probe directly the electronic structure of solids with atomic resolution. However, to the best of our knowledge, irradiated NTs have not been yet studied by STM.

Inasmuch as the interpretation of STM images and, in particular, the determination of defect-induced features in experimental STM images is not straightforward due to various electronic effects, in this paper we simulate STM images of NTs with single vacancies. Our main goal here is to facilitate the interpretation of possible experimental STM

* Present address: Accelerator Laboratory, P.O. Box 43, FIN-00014, University of Helsinki, Finland.

E-mail address: akrashen@beam.helsinki.fi (A.V. Krasheninnikov).

0038-1098/01/$ - see front matter
PII: S0038-1098(01)00109-0

images of irradiated NTs and to clarify: (i) Can STM detect single vacancies (if they exist) on walls of NTs? (ii) How do such vacancies affect STM images of NTs? We suggest that vacancies are created upon irradiating NTs with, e.g., low-energy ($\leq$100 eV) ions of inert gases. We neither model the impact event here nor address the issue of vacancy stability; this will be done elsewhere [13].

We demonstrate for the first time that vacancies result in the formation of hillock-like features in the STM images of metallic NTs. The characteristic lateral size of the hillocks is about 5 Å, whereas their height is up to 1 Å. Thus, vacancies may be detected by STM. Electronic superstructures (SSs) analogous to those in graphite near point defects are observed near vacancies. For semiconducting NTs, hillocks and SSs are also observable at those bias voltages when band-edge states contribute to the tunneling current.

In calculating STM images of NTs with vacancies, we generally adopt the Green's-function technique used in Refs. 14 and 15 to simulate STM images of graphite surfaces within the tight-binding (TB) approximation. The validity of the TB approach for calculating electronic and mechanical properties of NTs has been confirmed many times by ab initio calculations [2,16,17]. Our approach is close to that used in Ref. 18 for simulations of the STM images of perfect NTs. To verify our approach, we calculated STM images of NTs without defects. Our results agree well with both simulated [2,3,18] and experimental [19,20,21] images.

In calculations of the atomic network relaxation near the vacancy we employ the four-band TB Hamiltonian [23] which accounts for electron hopping beyond the first-neighbor approximation. However, since the electronic structure of single-wall NTs near the Fermi energy is governed by the π-states oriented perpendicularly to the NT walls, we take into consideration only these states in calculations of STM images. To the first order in the tip-NT interaction, the tunneling current I as a function of the tip coordinates (x,y,z) may be written at zero temperature as

$$I(x,y,z) = \frac{2\pi e}{\hbar}\int_0^{eV_{\rm bias}} \sum_i |V_i(x,y,z)|^2 \rho_{tip}(E)\rho_{\rm tube}(i,E)dE, \quad (1)$$

where the sum runs over all sites involved in the tip-NT hopping. $V_{\rm bias}$ is the bias voltage applied to the tip-NT interface, $V_i(x,y,z)$ is the tunneling matrix element coupling the tip apex atom to the atom i of the NT, $\rho_{\rm tip}(E)$ and $\rho_{\rm tube}(i,E)$ are the local densities of states (LDOS) of the noninteracting tip and the NT, respectively. Note that the equation (1) has an approximate character; however, its applicability for calculating STM images of carbon systems has been demonstrated [14,15]. The tip was modelled as a semi-infinite chain of atoms. The parameter V was evaluated numerically with the tip states being approximated by a hydrogen-like d-function mimicking a tungsten tip. The recursion method [24,25] was employed to calculate LDOS of a NT. STM images were computed for the constant current mode of STM operation, in which the height of the STM tip is adjusted to keep a constant value of current. To simulate this mode, we numerically solved the equation (cur) for the z coordinate (tip height $h \equiv z$) at any scan point (x,y). Other details of our calculations will be given elsewhere [13].

Inasmuch as we are interested in what is taking place in the electronic structure of NTs upon vacancy formation and since the change is most dramatic for the states near E_F (as we show below), we take for metallic NTs small bias voltages $V_{\rm bias} = 0.2$ V. Thus, only electronic states near E_F contribute to the tunneling current. We account for the shift [22] of E_F by $\delta E = 0.3$ eV due to the charge transfer from the substrate, which leads to an asymmetric position of the NT band structure relative to E_F, see Fig. 2(b).

We start with metallic (15,0) NTs. Let us postulate that a vacancy is formed in the topmost part of a NT. Having calculated the relaxation of the carbon network near the vacancy, we computed STM images of the NT.

Figs. 1(a,b) present isometric plots of the variation in tip height h for a scan across (x,y) near the vacancy (which is at the origin) for $V_{\rm bias} = \pm 0.2$ V. A dramatic protrusion above the vacancy is evident. The height of the hillock constitutes ≈ 0.7 Å (0.5 Å) for the positive (negative) value of $V_{\rm bias}$, while its linear size is independent of the sign of $V_{\rm bias}$ and constitutes ≈ 5 Å. To achieve atomic corrugation, we

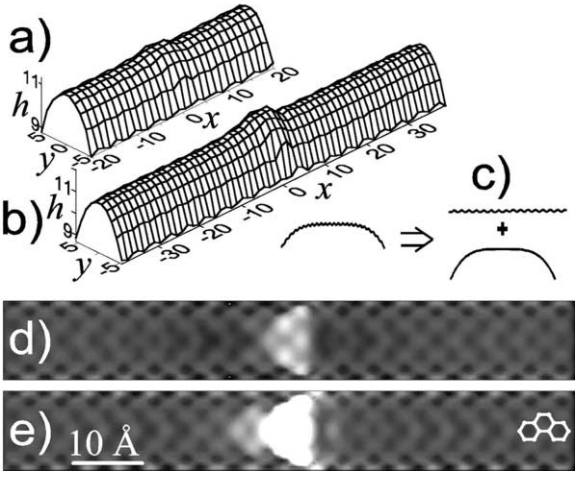

Fig. 1. STM image of a (15,0) metallic NT with a vacancy. (a) Isometric plot of tip height h as a function of tip position in the (x,y) plane for $V_{\rm bias} = -0.2$ V. (b) The same as in (a), but for $V_{\rm bias} = +0.2$ V. (c) Illustration for achieving atomic corrugation ("filtering" the STM image) by subtracting the averaged (over the NT axis x) profile of the NT. (d,e) Filtered gray-scale STM images for $V_{\rm bias} = -0.2$ V (d) and $V_{\rm bias} = +0.2$ V (e). All lengths are given in Angstroms. The vacancy is at the origin in the (x,y) plane (at the centers of the images). A part of the NT carbon network is also sketched.

subtract the profile of the NT averaged over its axis from the initial profile (Figs. 1(a,b)), as illustrated in Fig. 1(c). Figs. 1(d,e) depict the filtered STM image of the central part of the NT for positive and negative V_{bias}. It is seen that the hillock has a trigonal form and that the hillock orientation is governed by that of the atoms in the NT carbon network.

To understand the origin of the hillock, in Fig. 2(a) we plot current-to-voltage (I–V) characteristic for the tip positioned above the vacancy. The I–V curve is actually the LDOS on carbon atoms surrounding the vacancy and contributing to the tunneling current. In Fig. 2(b) we plot the I–V curve calculated at a distance from the vacancy, and this coincides with the I–V curve for a defect-free NT. As evident from the figures, the vacancy results in a sharp increase in LDOS near E_F on atoms nearest the vacancy.

Besides a hillock-like feature, it can also be seen from Figs. 1(d,e) that the STM image of the NT in the vicinity of the vacancy is different from that calculated at a distance from the defect. A network of dark spots corresponding to the centers of hexagons is evident at the ends of the images, whereas modulations in h along the NT axis are present near the vacancy. The amplitude of these modulations, or superstructure (SS), decreases with the distance from the vacancy.

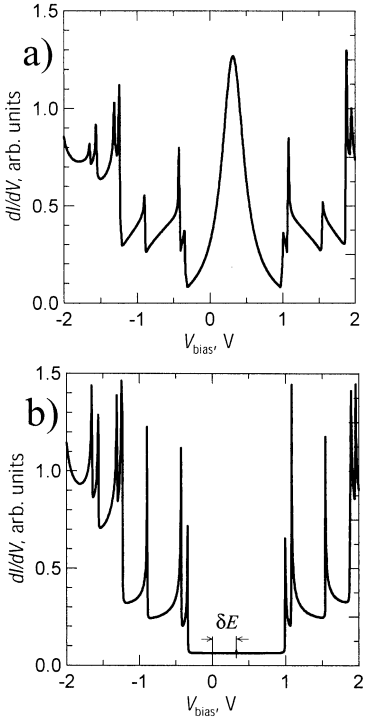

Fig. 2. I–V curves for the (15,0) NT calculated just above the vacancy (a) and above an atom distanced from the defect (b). Zero voltage corresponds to the position of E_F, δE is the shift of E_F due to the charge transfer from the substrate.

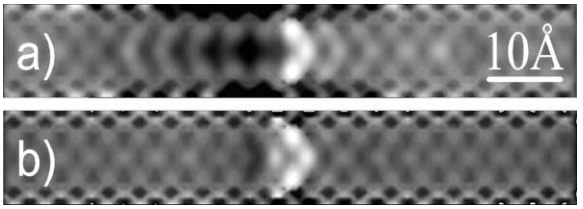

Fig. 3. STM gray-scale image of a semiconducting (14,0) NT with a vacancy. (a) $V_{bias} = -0.4$ V (b) $V_{bias} = +0.4$ V. The vacancy is at the centers of the images.

Note that we did not find any re-arrangement of atoms in the NTs after geometry optimization. Thus, the hillock and the SS have a purely electronic origin.

Now we proceed to semiconducting NTs. Fig. 3(a) presents an STM image of the central part of a (14,0) NT with a single vacancy for positive and negative values of $V_{bias} = \pm 0.4$ V. As follows from these figures, vacancies in semiconducting NTs also change the STM images, resulting in the formation of hillock-like features and SSs near the defect. However, the heights of the hillocks are ≈ 0.3 Å, which is less than that for metallic NTs.

For semiconducting NTs, the hillocks and SSs stem from changes in the LDOS on atoms in the vicinity of the vacancies for energies corresponding to the band edges at the semiconductor gap, see also Fig. 4, in which I–V curves just above and at a distance from the vacancy are shown. A

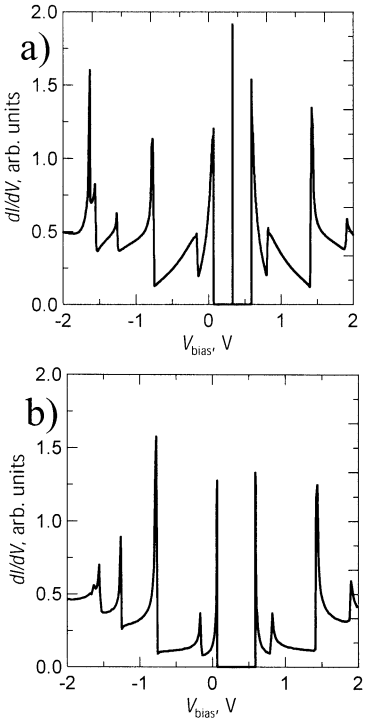

Fig. 4. The same as in Fig. 2, but for the (14,0) NT.

vacancy also results in the formation of dispersionless peaks at E_F in the LDOS of atoms near the vacancy, see Fig. 4(a). However, the contribution of these states to the tunneling current is very small.

Qualitatively similar results are obtained for all (not only zigzag) metallic and semiconducting NTs with various indices. Vacancies always result in the appearance of hillocks and SSs, the size and orientation of which sensitively depend on the NT chirality. Here, we also stress that when we account for next-nearest-neighbor hopping, SSs may be different for positive and negative V_{bias}, which agrees with the data from a recent theoretical work, [26] where appearances of such features in STM images of NTs near point defects have been reported as well.

The main features in STM images of NTs with vacancies—hillocks and SSs—have also been reported for experimental STM images of graphite surfaces with vacancies, [27,28] although such features in graphite may result not only from vacancies, but also from interstitial atoms below the surface[29].

The STM images which we have calculated for NTs and STM images of graphite surfaces with vacancies have much in common. In particular, the dimensions of hillocks, their trigonal form, and the form of SSs are all nearly identical in both cases. As follows from theoretical simulations carried out within a framework of a tight-binding approximation [15,31,32] and first-principles plane-wave formalism, [30,33] the features predicted for STM images of NTs and observed for graphite have one and the same physical origin. Thus, our results for NTs, if corroborated experimentally, may not only shed light on the existence of vacancies in NTs, but may also confirm the presence of vacancy-induced hillocks in STM images of graphite as well as help identify the actual type of point defect which has resulted in a particular feature.

To conclude, we calculated STM images of both metallic and semiconducting single-wall carbon NTs with atomic vacancies. We predict that vacancies should result in the formation of hillock-like features in STM images of NTs, which are especially appreciable at small $V_{\text{bias}} \approx 0.1$–$0.4$ V. Depending on the NT chirality, the characteristic lateral size of the hillocks is about 5–8 Å, whereas their height is up to 1 Å. Thus, vacancies may be detected by STM. The enhancement in the tunneling current is due to the increase in LDOS for the states at the Fermi energy, which are spatially localized on the atoms surrounding the vacancies (and may be also interpreted as "dangling bonds"). Electronic superstructures analogous to those in graphite near point defects are observed near the vacancy.

Acknowledgements

I greatly benefited from discussions with K.H. Nordlund, R.M. Nieminen, S.N. Molotkov, V.F. Elesin, L.A. Openov, K. Eltsov and D. Cannon. I would also like to thank Elsevier Science Publishing for giving me a one-year free subscription to Surface Science. This work was supported by the Russian Federal Program "Integration" (Project No AO133).

References

[1] D. Orlikowski, M.B. Nardelli, J. Bernholc, C. Roland, Phys. Rev. B61 (2000) 14194.
[2] A. Rubio, Applied Physics A68 (1999) 275.
[3] J.-C. Charlier, T.W. Ebessen, Ph. Lambin, Phys. Rev. B53 (1996) 11108.
[4] Y. Xia, Y. Ma, Y. Xing, Y. Mu, C. Tan, L. Mei, Phys. Rev. B61 (2000) 11088.
[5] L. Chico, L.X. Benedict, S.G. Louie, M.L. Cohen, Phys. Rev. B54 (1996) 2600.
[6] A. Hansson, M. Paulsson, S. Stafström, Phys. Rev. B62 (2000) 7639.
[7] M. Igami, T. Nakanishi, T. Ando, Physica B 284-288 (2000) 1746.
[8] H.J. Choi, J. Ihm, S.G. Louie, M.L. Cohen, Phys. Rev. Lett. 84 (2000) 2917.
[9] T. Kostyrko, M. Bartkowiak, G.D. Mahan, Phys. Rev. B60 (1999) 10735.
[10] C.-H. Kiang, W.A. Goddard, R. Beyers, D.S. Bethune, J. Phys. Chem. 100 (1996) 3749.
[11] P.M. Ajayan, V. Ravikumar, J.-C. Charlier, Phys. Rev. Lett. B81 (1998) 1437.
[12] Y. Zhu, T. Yi, B. Zheng, L. Cao, Appl. Surf. Sci. 137 (1999) 83.
[13] A.V. Krasheninnikov, K. Nordlund, M. Sirviö, E. Salonen, J. Keinonen, Phys. Rev. B (2001) in press.
[14] B.A. McKinnon, T.C. Choy, Phys. Rev. B54 (1996) 11777.
[15] A.V. Krasheninnikov, V.F. Elesin, Surf. Sci. 454-456 (2000) 519.
[16] E. Hernández, C. Goze, P. Bernier, A. Rubio, Phys. Rev. Lett. 80 (1998) 4502.
[17] D. Östling, D. Tománek, A. Rosén, Phys. Rev. B55 (1997) 13980.
[18] V. Meanier, Ph. Lambin, Phys. Rev. Lett. 81 (1998) 5588.
[19] J.W.G. Wildöer, L.C. Venema, A.G. Rinzler, R.E. Smalley, C. Dekker, Nature 391 (1998) 59.
[20] T.W. Odom, J.L. Huang, P. Kim, C.M. Lieber, Nature 391 (1998) 62.
[21] L.C. Venema, V. Meunier, Ph. Lambin, C. Dekker, Phys. Rev. B61 (2000) 2991.
[22] L.C. Venema, J.W. Janssen, M.R. Buitelaar, J.W.G. Wildöer, S.G. Lemay, L.P. Kouwenhoven, C. Dekker, Phys. Rev. B62 (2000) 5238.
[23] C.H. Xu, C.Z. Wang, C.T. Chan, K.M. Ho, J. Phys.: Condens. Matter 4 (1992) 6047.
[24] R. Haydoc, Solid State Phys. 35 (1980) 216.
[25] C.M. Goringer, D.R. Bowler, E. Hernández, Rep. Prog. Phys. 60 (1997) 1447.
[26] C.L. Kane, E.J. Mele, Phys. Rev. B59 (1999) R12759.
[27] J.R. Hahn, H. Kang, Phys. Rev. B60 (1999) 6007.
[28] J.G. Kushmerick, K.F. Kelly, H.-P. Rust, N.J. Halas, P.S. Weiss, Phys. Chem. B103 (1999) 1619.
[29] S. Habenicht, W. Bolse, H. Feldermann, U. Geyer, H. Hofsäss,

K.P. Lieb, F. Roccaforte, Europhys. Lett. 50 (2000) 209 and references therein.
[30] K. Nordlund, J. Keinonen, T. Mattila, Phys. Rev. Lett. 77 (1996) 699.
[31] K.F. Kelly, N.J. Halas, Surf. Sci. 416 (1998) L1085.
[32] M. Hjort, S. Stafström, Phys. Rev. B61 (2000) 14089.
[33] N. Takeuchi, J. Valenzuela-Benavides, L. Morales de la Garza, Surf. Sci. 380 (1997) 190.